NASA TECHNICAL MEMORANDUM

NASA TM-82518

GRAVITY PROBE-B CONTROL SUBSYSTEM

By John Farmer
Systems Dynamics Laboratory

January 1983

NASA

George C. Marshall Space Flight Center
Marshall Space Flight Center, Alabama

MSFC - Form 3190 (Rev June 1971)

TECHNICAL REPORT STANDARD TITLE PAGE

1. REPORT NO.	2. GOVERNMENT ACCESSION NO.	3. RECIPIENT'S CATALOG NO.
NASA TM-82518		

4. TITLE AND SUBTITLE	5. REPORT DATE
Gravity Probe-B Control Subsystem	January 1983
	6. PERFORMING ORGANIZATION CODE
7. AUTHOR(S)	8. PERFORMING ORGANIZATION REPORT #
John Farmer	
9. PERFORMING ORGANIZATION NAME AND ADDRESS	10. WORK UNIT NO.
George C. Marshall Space Flight Center Marshall Space Flight Center, Alabama 35812	11. CONTRACT OR GRANT NO.
	13. TYPE OF REPORT & PERIOD COVERED
12. SPONSORING AGENCY NAME AND ADDRESS	Technical Memorandum
National Aeronautics and Space Administration Washington, D.C. 20546	14. SPONSORING AGENCY CODE

15. SUPPLEMENTARY NOTES

Prepared by Systems Dynamics Laboratory, Science and Engineering Directorate.

16. ABSTRACT

The purpose of this document is to identify and briefly examine the control problems of the proposed Gravity Probe-B spacecraft. Suggestions are made for control thruster geometry, dynamics, and maximum output value. Maximum total thrust is also a consideration since all thrusters expel gaseous helium produced from a common liquid supply. Control philosophy and preliminary designs are presented for both the attitude and drag free control systems. A radial separation of the spacecraft center of mass and the center of the proof mass cavity produces cross coupling between the attitude and drag free systems. The low available thrust implies that this separation, throughout the mission, must be kept within very close tolerance. For this reason an on-board mass balance control system may be necessary.

Simulation was performed only to the extent necessary to show the control concepts to be feasible.

17. KEY WORDS	18. DISTRIBUTION STATEMENT
Attitude control, thruster, drag free control, boil-off control, sensors, aerodynamic, centrifugal, digital computer, response, operational mode, telescope, liquid helium, mass balance, inner gimbal control, control law	Unclassified – Unlimited

19. SECURITY CLASSIF. (of this report)	20. SECURITY CLASSIF. (of this page)	21. NO. OF PAGES	22. PRICE
Unclassified	Unclassified	45	NTIS

PRECEDING PAGE BLANK NOT FILMED

TABLE OF CONTENTS

LIST OF ILLUSTRATIONS

LIST OF TABLES

TECHNICAL MEMORANDUM

GRAVITY PROBE-B CONTROL SUBSYSTEM

INTRODUCTION AND GENERAL CONTROL REQUIREMENTS

The instrument package of the Gravity Probe-B spacecraft is surrounded by a mass of liquid helium which over the lifetime of the vehicle gradually "boils away" to produce helium gas. The venting of this gaseous helium through selected thrusters provides the forces necessary for spacecraft control.

Onboard sensors provide the appropriate signals for attitude and drag-free control. The effect of the flexible body characteristics of the four solar arrays and the instrument suspension must be adequately damped by the attitude control system to insure desired stability margins. Control design must account for the effects of liquid helium sloshing and any cross-coupling between the various vehicle control systems.

Attitude control will be maintained throughout the one-year scientific data taking phase of the mission as well as the period allowed for preparation, i.e., gyro spin-up, spacecraft spin-up, etc. Drag-free control must be achieved for a minimum of 95 percent of the time when scientific data is available.

Present studies indicate that the onboard control systems needed to accomplish the mission requirements include:

1) Attitude Control System.

2) Drag-Free Control System.

3) Inner Gimbal (subject of trade study).

4) Mass Balance (operated open loop).

5) Helium Boil-off Control.

THRUSTER GEOMETRY

Sixteen variable thrusters are used for attitude and drag-free control of the spacecraft. A thruster pod arranged as shown in Figure 1 is located at the tip of each solar array. The propulsive helium gas is delivered to each pod by means of an aluminum pipe which remains fixed as the solar arrays are articulated.

By firing the appropriate thruster, torques for attitude control can be developed about any arbitrary vehicle axis and translation forces for drag-free control can be achieved in any direction. This thruster arrangement is one of the more obvious configurations and provides for simple thruster selection control logic with some failure mode redundancy.

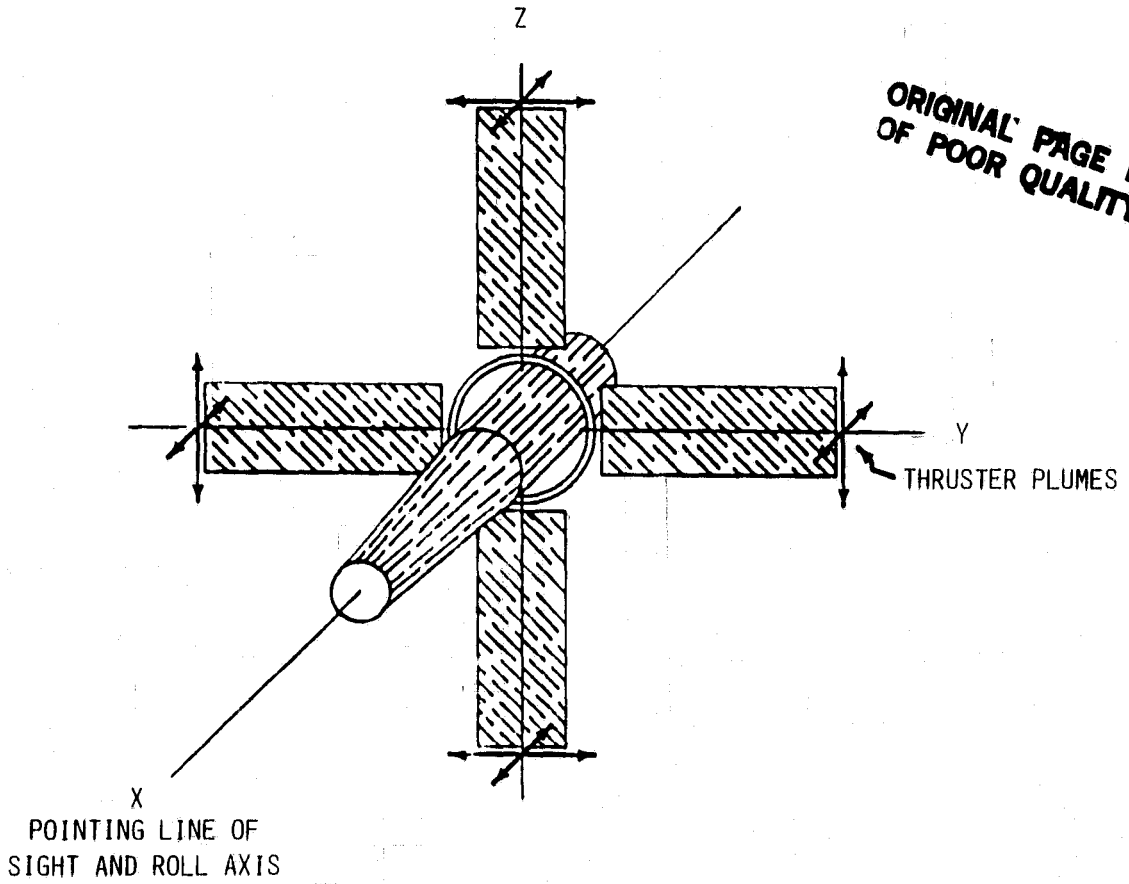

Figure 1. Thruster geometry.

Further work should be done in this area to insure that a more efficient thruster mounting geometry does not exist. This study should examine existing literature and involve trades concerning the number of thrusters needed, plume impingement, failure modes, and control law complexity.

THRUSTER SIZING

From the beginning of this study, the atmospheric forces have been the driving factor in determining the maximum thruster output. These atmospheric drags and torques are strongly influenced by the expected solar activity and, therefore, the vehicle launch date.

Uncertainties in launch date, solar activity, and atmospheric data call for a conservative approach to sizing the control thrusters. The maximum expected demand on the thrusters in each vehicle axis was first estimated. The worst case was then chosen, a 10 percent contingency added, and all thrusters sized to this value.

Aerodynamic drags and torques are shown superimposed on the vehicle axes in Figure 2. The forces and moments are shown with their positive sense and are defined by equation (1).

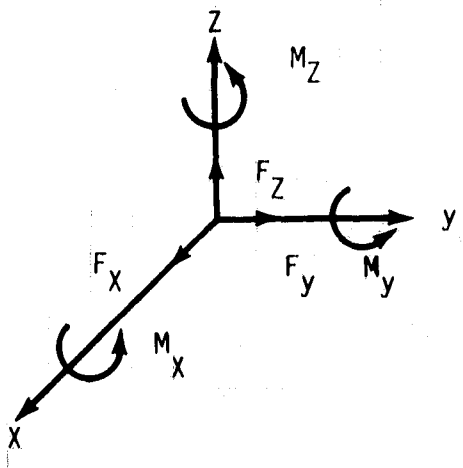

Figure 2. Aerodynamic drags and torques.

$$F_x = -\frac{1}{2}\rho V^2 C_A A_{REF} \qquad M_x = +\frac{1}{2}\rho V^2 C_{MR} A_{REF} L_{REF}$$

$$F_y = -\frac{1}{2}\rho V^2 C_Y A_{REF} \quad ; \quad M_y = -\frac{1}{2}\rho V^2 C_{MP} A_{REF} L_{REF} \qquad (1)$$

$$F_z = +\frac{1}{2}\rho V^2 C_N A_{REF} \qquad M_z = -\frac{1}{2}\rho V^2 C_{MY} A_{REF} L_{REF}$$

where

ρ = atmospheric density (Kg/m^3).

V = spacecraft velocity (m/s).

A_{REF} = reference area (m^2).

L_{REF} = reference lever arm (m).

C_A, C_Y, C_N = drag force coefficients (unitless).

C_{MR}, C_{MP}, C_{MY} = pitching moment coefficients (unitless).

Table 1 shows the worst case drag and moment coefficients. The maximum sum in this table represents that vehicle orientation which produced the greatest sum of the individual drag coefficients and does not indicate the addition of the values tabulated.

Assuming the maximum atmospheric density, a vehicle velocity associated with a 520 km orbit and the maximum drag and torque coefficients the worst case force and moment values for each vehicle axis can be computed. These values are shown in Table 2.

TABLE 1. WORST CASE DRAG AND MOMENT COEFFICIENTS

Solar Array Angle		0°	90°
x-axis	C_A	2.08	4.75
y-axis	C_N	3.323	2.39
z-axis	C_Y	3.323	2.391
max-sum (force coeff.)		6.132	6.781
x-axis	C_{MR}	0.039	0.019
y-axis	C_{MP}	0.178	0.182
z-axis	C_{MY}	0.178	0.187

TABLE 2. WORST CASE FORCE AND MOMENT VALUES

Vehicle Axis	Drag Force (N)	Aerodynamic Torque (N-m)
x	144.9×10^{-4}	4.6×10^{-4}
y	101.4×10^{-4}	21.45×10^{-4}
z	72.9×10^{-4}	22.04×10^{-4}

Maximum forces and torques causing thruster firings parallel to all vehicle axes were calculated. Included in these torques were nutation, gravity gradient, drag-free coupling, centripetal, dither, and control. Summing all forces and torques produces the values in Table 3.

TABLE 3. SUMMATION OF ALL FORCES AND TORQUES

Vehicle Axis	Total Force (N) (+10% Contingency)	Number of Thrusters	Force per Thrusters (N)
x	171.16×10^{-4}	4	42.79×10^{-4}
y	130.2×10^{-4}	2	65.1×10^{-4}
z	98.48×10^{-4}	2	49.24×10^{-4}

Each axial force requirement must be modified by the number of thrusters available to produce that force. Since the y vehicle axis produces the greatest value, all thrusters will be sized to give a maximum value of

$$F_{MAX} = 65 \times 10^{-4} \text{ N} \quad .$$

The thrusters are sized in a manner which deals only with the maximum disturbances expected. Impingement forces have not been included in this analysis. However, they are expected to be less than 5 percent and should be accounted for in the contingency.

PEAK AND AVERAGE FORCE REQUIREMENTS

The normal heat leak into the dewar causes the liquid helium to transform into the propulsive helium gas needed for the individual thrusters. During the course of the one year mission, conditions may arise that call for more propulsive gas than is presently available. This is one purpose of the proposed boil-off control system – to insure that the propulsive gas is available when needed for attitude and drag-free control.

The maximum amount of thrust required must include the simultaneous requirement in all three vehicle axes. The maximum sum of force coefficients occurs when the solar arrays are at 90° as shown in Table 1. Averaging the force coefficients and summing the averages gives the following values:

$$C_{MAX} = 6.781 \quad ; \quad C_{AVG} = 4.95 \quad .$$

Figure 3 shows the maximum orbital density as a function of cumulative frequency and is representative of the time frame in which the GP-B mission was scheduled. Values read from the solid curve indicate the time that the maximum atmospheric density would be equal to or less than the value shown (e.g., 50 percent of the time the maximum density is less than or equal to 2.5 x 10^{-12} kg/m^3). Realistically these values occur only once per orbit and on the average are much less than the maximum values shown. The dashed line in Figure 3 represents these average values and is more meaningful in estimating the average thruster force required over the entire mission.

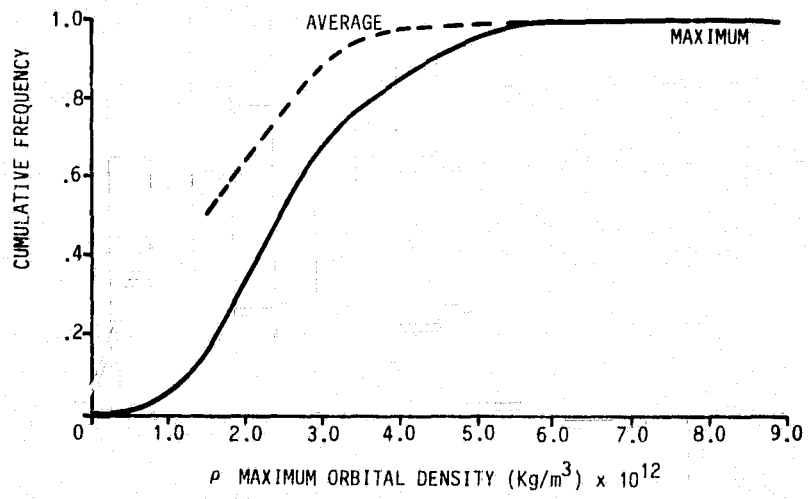

Figure 3. Atmospheric density.

Using the average density over the orbit, the total force (sum of the force requirement in all vehicle axes) is calculated for the maximum and average values of aerodynamic force coefficients. These values are tabulated in Table 4.

TABLE 4. MAXIMUM AND AVERAGE AERODYNAMIC FORCE COEFFICIENTS

Cumulative Frequency	100%	99%	95%	50%
$F_{TOTAL}(C_{MAX} = 6.781)N$	177.88×10^{-4}	130.48×10^{-4}	96.48×10^{-4}	55.08×10^{-4}
$F_{TOTAL}(C_{AVG} = 4.95)N$	134.98×10^{-4}	100.08×10^{-4}	75.28×10^{-4}	45.08×10^{-4}

The average heat leak into the dewar is expected to produce enough propulsive gas to supply a constant thrust of

$$F_{TOTAL} = 98.7 \times 10^{-4} N \quad .$$

This amount of thrust is sufficient to maintain the attitude and drag-free control systems 95 percent of the time – even when the maximum drag coefficient sum is assumed.

The maximum boil-off point is defined as the point at which the control system is producing the maximum amount of propulsive helium gas. This point has been chosen at the 99 percent level where

$$F_{TOTAL} = 130 \times 10^{-4} N \quad .$$

This maximum point can be varied easily simply by making more power available to the boil-off heater.

A better definition of thruster size as well as peak and average force requirements may be affected by a statistical analysis of the available data. This approach should be undertaken as the design matures. However, so many uncertainties exist at this stage that a conservative and simpler approach was used. It is expected that the values chosen will in the final analysis meet any control need that may arise during the one year mission.

TORQUE ALLOCATIONS

The x vehicle axis (pointing axis) must be rotated to point at the guide star in the acquisition and reacquisition modes of operation. The torque (T) needed to rotate the vehicle is applied in the inertial frame and lies in the plane of the Y-Z vehicle axes. The spacecraft may or may not be spinning about the pointing axis – in either case it is possible for the torque vector to assume various angular positions in the vehicle coordinate frame. The pointing control system must provide the total torque by torqueing each vehicle axis as shown in Figure 4.

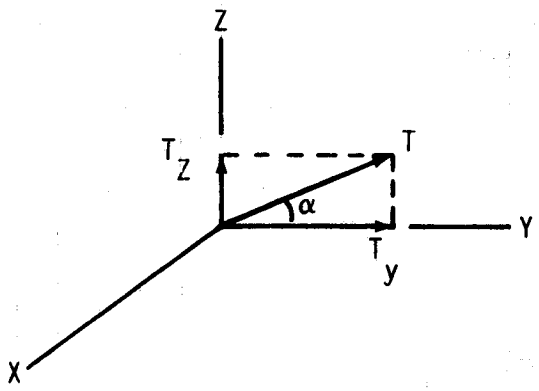

Figure 4. Torque components in vehicle frame.

The worst case, from the standpoint of utilizing the maximum amount of vehicle torque occurs when $\alpha = 45$ deg. To achieve the control torque (T) the vehicle control system must produce

$$T_V = T_Y + T_Z = T \cos \alpha + T \sin \alpha = 1.414\, T \quad . \tag{2}$$

The GP-B spacecraft is severely torque limited. The sum of the outputs of all thrusters cannot exceed $F_{MAX} = 0.013$ N at any time. The maximum allowable vehicle torque can be expressed as

$$T_V = F_{MAX}\, L\, P_C \quad , \tag{3}$$

where

L = thruster lever arm (m)

P_C = fraction of maximum thrust allotted to maneuvering (unitless).

Due to overshoot in the control system and the fact that other external torques (gravity gradient, nutation, etc.) must be accounted for, it is recommended that P_C not exceed 40 to 50 percent. Using equations (2) and (3) the maximum allowable inertial torque is given by

$$T = \frac{T_V}{1.414} = \frac{F_{MAX}\, L\, P_C}{1.414} \tag{4}$$

ATTITUDE CONTROL SYSTEM (ACS)

For a successful mission the ACS must perform in several different modes of operation. Each mode of operation and the requirements for that particular mode will be discussed.

Acquisition

The ACS must acquire the guide star Rigel after being released by the Shuttle Remote Manipulator System (RMS). Vehicle angular rate signals for control during this period will be obtained from redundant rate gyroscopes in all vehicle axes. Pointing error information will be processed in the flight control computer from three possible sources – sun sensors, star trackers, and the instrument telescope. The sun sensors and star trackers will be used only for the purpose of bringing the guide star into the telescope field-of-view. The spacecraft has no spin rate and, therefore, no momentum vector that must be rotated as pointing is accomplished. The pointing accuracy in this mode and all other modes is defined by the linear range of the telescope which is presently ±0.05 arc sec in the pitch and yaw vehicle axes. The drag-free control system is not active during initial acquisition.

For large angle maneuvers, a reference frame rate will be generated and input to the control algorithm. The reference frame rate is assumed to have a sinusoidal shape as shown in Figure 5. The vehicle reference frame accelerates about some axis of rotation through one-half of the total angle and slows through the remaining half.

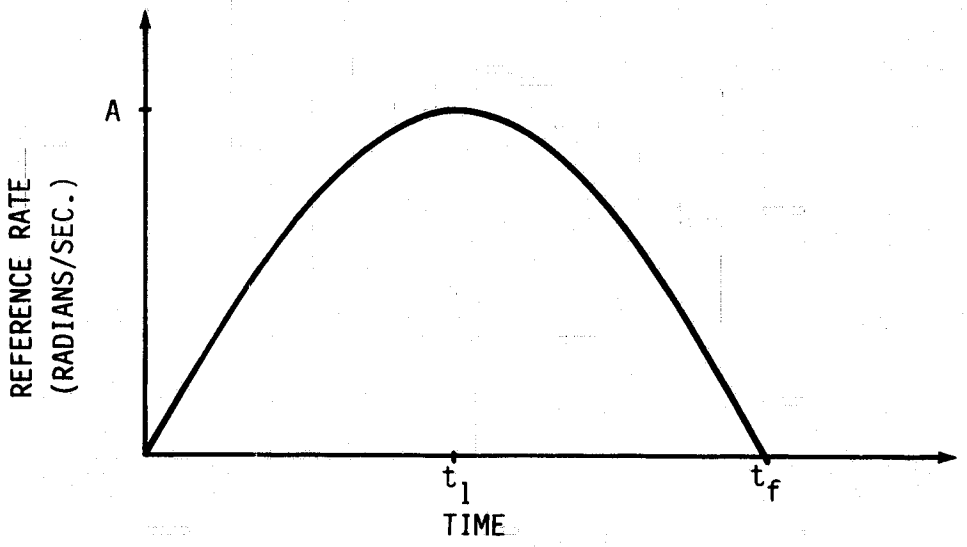

Figure 5. Reference frame rate command.

The reference frame rate is described by

$$\omega_R = A \sin \omega_N t \quad , \tag{5}$$

where

A = amplitude of the half sine wave (rad/sec)

$t_f = 2t_1$ = one half of the period (sec)

$\omega_N = \pi / t_f$ = radian frequency (rad/sec).

Since the vehicle is not spinning, Eulers rotation equation reduces to

$$T = I\ \dot{\omega}_R = A\ I\ \omega_N \cos \omega_N t \quad , \tag{6}$$

where I is the moment of inertia about the torque axis. The torque is maximum at t = 0 and is given by

$$T = A\ I\ \omega_N \quad . \tag{7}$$

Therefore

$$A = \frac{T}{I\ \omega_N} \quad . \tag{8}$$

Substituting the definition of ω_N into equation (8) produces

$$A = \frac{T\ t_f}{I\ \pi} \quad . \tag{9}$$

If the angle of rotation is θ then

$$\theta = \int_o^{t_f} A \sin \omega_N t = \frac{2A}{\omega_N} = \frac{2A\ t_f}{\pi} \quad , \tag{10}$$

and

$$A = \frac{\pi\ \theta}{2t_f} \quad . \tag{11}$$

Equating (9) and (11) yields

$$t_f = \pi \left[\frac{I\theta}{2T}\right]^{1/2} \quad . \tag{12}$$

Substituting equation (12) into equation (9) produces the amplitude

$$A = \left[\frac{T\theta}{2I}\right]^{1/2} . \tag{13}$$

Also

$$\omega_N = \frac{\pi}{t_f} = \left[\frac{2T}{I\theta}\right]^{1/2} . \tag{14}$$

Using the value of T as determined by equation (4) with $P_C = 0.5$ and $P_C = 1.0$, the time to complete a maneuver can be computed for various angles of θ and plotted as shown in Figure 6.

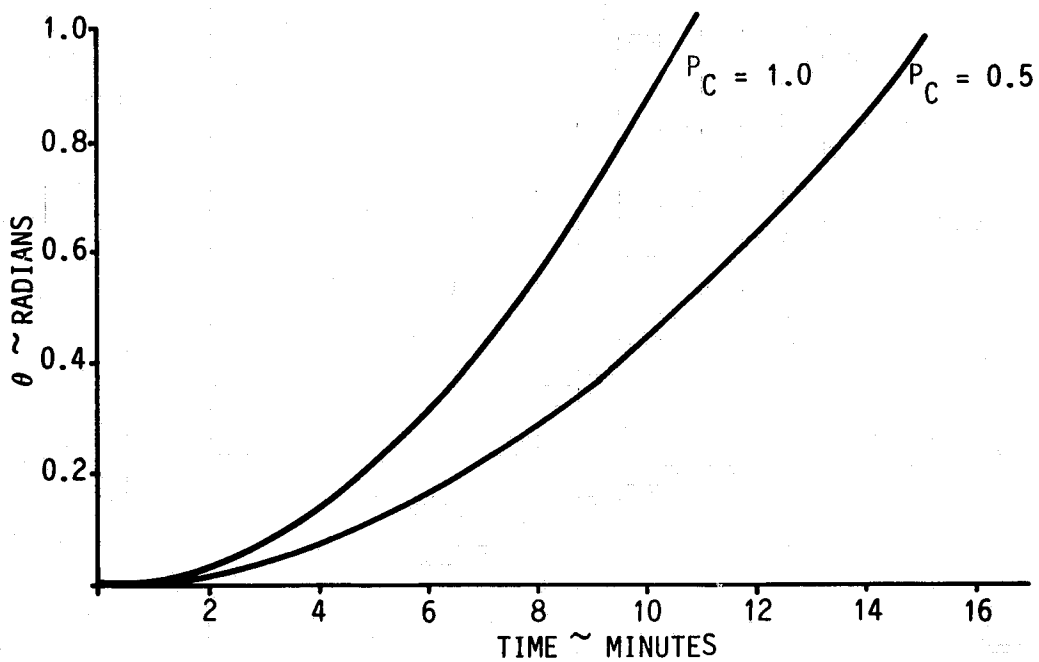

Figure 6. Pointing time requirement for acquisition mode.

The above equations characterize the reference frame movement, but will be closely approximated by the vehicle response which involves thrusters, control algorithms, etc.

Relativity Gyroscope Spin-Up

The experiment gyroscopes are brought up to speed by exhausting helium gas through a body fixed spin-up channel. The gas is directed over the gyro ball and exits through non-propulsive vents located at the rear of the vehicle. During the spin-up period precautions must be taken to insure that the spin axis of each gyro ball is aligned (i.e., parallel) as closely as possible with the spin axis of the vehicle. Two methods have been suggested to accomplish this.

1. Fast Spin – After acquiring the guide star and before drag-free control has been activated, the attitude control system will be commanded to spin at a high rate about the vehicle pointing axis. After acquiring a constant spin rate about its x axis, the Euler equations of rotation reduce to

$$T_x = 0 \quad ; \quad T_y = I_{xz}\omega_x^2 \quad ; \quad T_z = -I_{xy}\omega_x^2 \quad , \tag{15}$$

where

T_n = torque applied about vehicle axis n (N-M)

I_{xz}, I_{xy} = products of inertia (kg-m^2)

ω_x = spin rate (rad/sec).

While other disturbance torques are acting on the vehicle during this period, the nutation torque becomes the dominant requirement as the spin rate is increased. If the assumption is made that

$$I_{xz} \approx I_{xy}$$

then the total nutation torque is

$$T_{NU} = T_y + T_z = 2I_{xz}\omega_x^2 \quad . \tag{16}$$

The nutation torque requirement as a function of spin rate is plotted in Figure 7. The maximum and average torques available are shown as dashed lines. The primary reason for the fast spin mode is to insure that any misalignment in the body fixed spin-up channel will be averaged out as the gyro balls are brought up to speed. In this manner the spin-up channel would complete as many cycles as possible during the actual relativity gyro spin-up and, therefore, align the spin vectors. All four gyros will spin-up simultaneously if this method is used, and final speed would be reached in the shortest period of time.

A secondary reason for the fast spin mode is to cause the liquid helium to "seat" in a symmetrical ring which places the proof mass location at the helium center of mass. A faster than nominal spin rate is needed to initially put the helium into this configuration, but the present studies indicate that the nominal spin rate of 0.1 RPM is sufficient to maintain the liquid shape. The spin rate needed to seat the helium is shown in Figure 8 as a function of ullage volume (i.e., the volume of the dewar not occupied by liquid helium).

At this stage of development, no study has been performed which indicates that a vehicle fast spin mode will actually align the vehicle and relativity gyroscope spin vectors. It seems practical that this would be the case, but no proof has yet been offered. For this reason a second method of achieving gyroscope spin-up has been suggested.

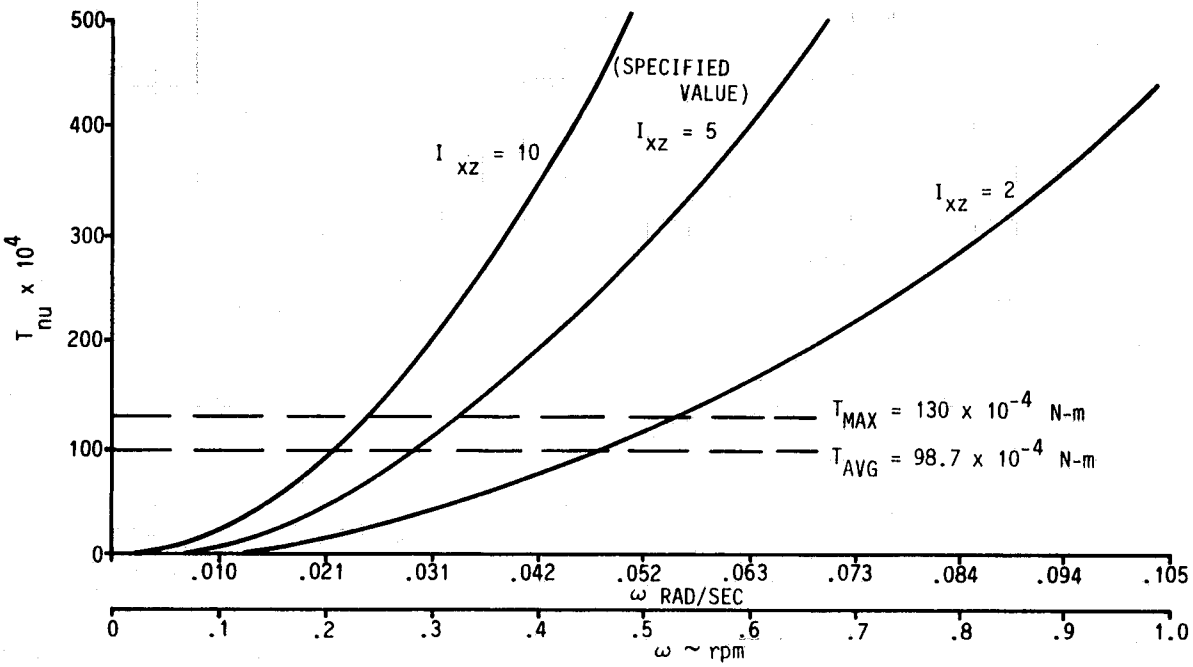

Figure 7. Nutation torque requirement.

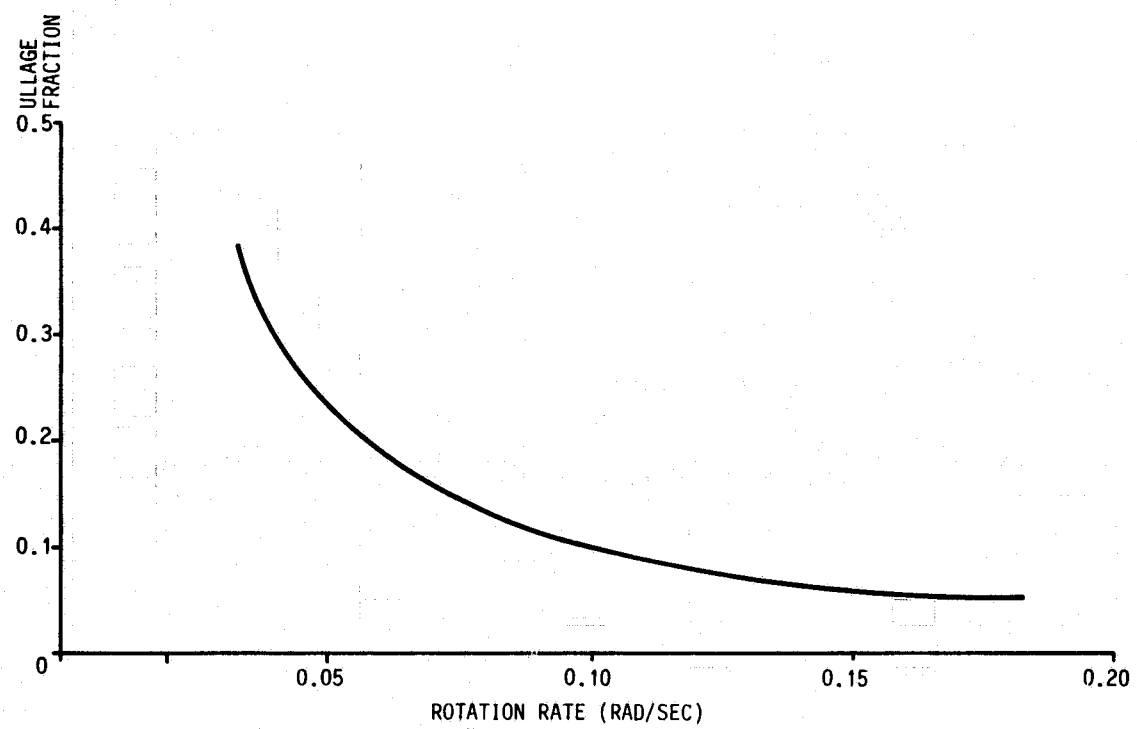

Figure 8. Ullage fraction versus rotation rate required for seating the liquid helium in the baffles.

2. Staged Spin-Up – This method requires more time to achieve final gyroscope speed, places a greater demand on the ACS and sequentially brings the gyro balls up to speed.

After release from the Shuttle, the guide star will be acquired in the normal manner. After acquisition, an accurate determination of the vehicle roll position will be made by the ACS. The ACS will be required to maintain this position while the gyroscopes are simultaneously brought up to some predetermined percentage of their final spin velocity. While holding this position enough orbits will be completed to allow the instrumentation to determine the direction of the individual gyroscope spin axes. Calculations may now be made which determine the vehicle roll angle which will more accurately align the spin vectors. A roll angular position will be calculated for each of the four gyroscopes and the spacecraft will in turn be positioned at these angles. At each position more helium gas will be exhausted to increase the gyro spin. A new spin vector will now be computed and the process will be repeated until each gyro has attained the required velocity and spin direction. The number of times this process must be completed has not been determined.

The non-propulsive exhausting of the spin-up gas is very important if this scenario is used. While venting, the spacecraft angular position must be accurately maintained by the ACS, which must null any residual torques produced by the venting gases.

This method does not eliminate the need for the fast spin mode since the liquid helium must be forced into the symmetrical shape discussed earlier. With this completed, the vehicle spin rate can now be decreased to its nominal value.

Drag-Free

Drag-free control is achieved by means of a proof mass which, for self-gravitation purposes, is located as close as possible to the center of mass of the total spacecraft. The proof mass is allowed to float freely within a cavity located inside the instrument. The body fixed location of the mass relative to the cavity center can be measured to an accuracy of one microinch. The mass location is used to generate commands to the appropriate control thrusters to translate the cavity center to keep the proof mass centered. In this manner, drag forces are countered by the thrusters and the spacecraft "follows," the proof mass in its drag-free environment. An average orbital acceleration of 10^{-10} g's is required to meet scientific goals. Average orbital acceleration is defined to be

$$A_{AVG} = \frac{\sum_{i=0}^{m} |a_i| \, \Delta\tau_i}{\sum_{i=0}^{m} \Delta\tau_i} = \frac{\sum_{i=0}^{m} |a_i| \, \Delta\tau_i}{T_o} \quad , \tag{17}$$

where

$|a_i|$ = acceleration magnitude of the vehicle center of mass (m/s^2).

$\Delta\tau_i$ = time interval for which a_i can be considered constant (s).

T_o = time to complete one orbit (s).

During fabrication of the spacecraft, an effort will be made to insure that the vehicle center of mass coincides with the center of the proof mass cavity and that the telescope line-of-sight passes through the same point. If the center of mass and proof mass do not coincide, then attitude control will be coupled to drag-free control and the resulting centrifugal forces must be countered by the control thrusters.

Consider the simplified case shown in Figure 9.

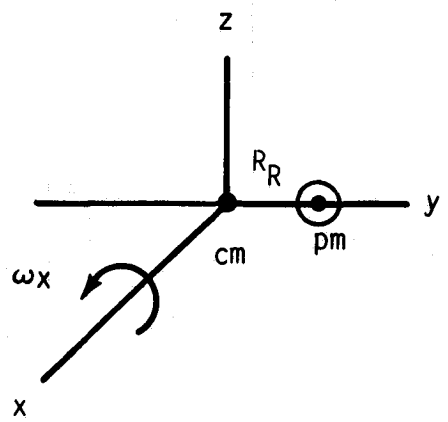

Figure 9. Simplified proof mass radial offset.

Attitude control commands to spin the vehicle about the x axis produce a movement of the proof mass cavity about the center of mass in a circular motion. The arc traversed by the cavity in time $\Delta\tau$ is given by

$$d_a = R_R \omega_x \Delta\tau \quad . \tag{18}$$

where

R_R = radial displacement of proof mass (m)

ω_x = vehicle spin rate (rad/sec).

The distance d_a represents a displacement of the proof mass and, through the drag-free control system, calls for a translational force to accelerate the vehicle and recenter the mass. The linear acceleration is given by

$$A = F/M_v \quad . \tag{19}$$

The force F in equation (19) is a combination of all forces acting to translate the vehicle and includes external as well as control thruster forces. This acceleration gives a cavity displacement of

$$d = \iint a \, d\tau \, d\tau \quad .$$

Combining the effects of the spinning vehicle and the translational forces effectively shifts the spin vector to pass through the center of the cavity and parallel to the x axis.

A new situation now exists with the center of mass rotating about the proof mass.. Centrifugal forces must now be cancelled by the control system as shown in Figure 10.

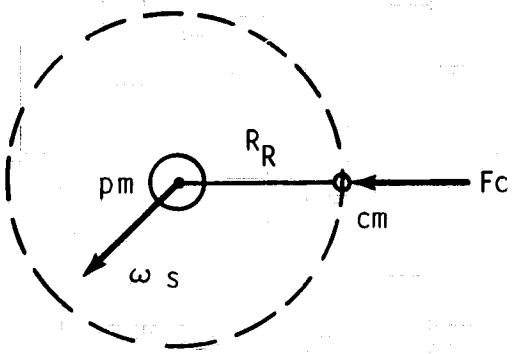

Figure 10. Centrifugal forces cancelled by ACS.

Centrifugal acceleration is directed toward the center of rotation and is determined by

$$a_c = \omega_s^2 R_R \quad , \tag{20}$$

the displacement of the cavity is

$$d_c = 1/2\ a_c\ \Delta\tau^2 \quad .$$

Body fixed forces (F_c in Fig. 10) must be developed by the thrusters to null the centrifugal forces and maintain the proof mass at its null position.

The total proof mass displacement is given by

$$R_o = -(d + d_a + d_c) \quad . \tag{21}$$

Where the negative sign arises from the fact that the mass displacement within the cavity is opposite the cavity movement. In the steady state the mass is centered, therefore,

$$R_o = 0 \quad ,$$

the spin vector passes through the cavity center and

$$d_a = 0 \quad .$$

The final configuration produces equal translational and centrifugal displacements of opposite sign

$$d = -d_c$$

producing the force F_c which rotates with the center of mass.

Figure 11 shows a more detailed view of the possible vehicle spin vector positions and the telescope line-of-sight (LOS) movement. Figure 11(a) shows the steady conditions for coincident proof mass cavity (PM) and vehicle center of mass (CM) locations. The line-of-sight also passes through the cavity center. Figure 11(b) assumes a line-of-sight misalignment and a separation between the PM and CM. The drag-free control system has not been activated and the vehicle will spin about the CM causing the LOS to rotate along the dashed line. Figure 11(c) shows the same conditions as in 11(b) but with an active drag-free controller. The centrifugal forces F_c are generated and the spin vector changes positions to pass through the PM center again causing the LOS to move around the dashed line.

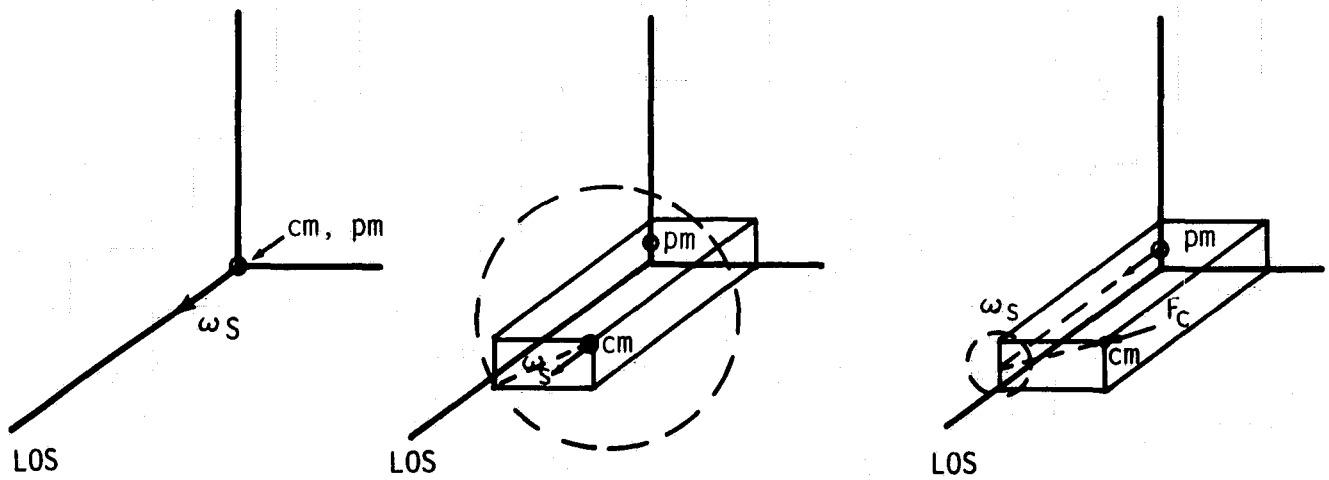

Figure 11. Vehicle spin vector position and LOS movement.

The question naturally arises concerning the maximum permissible value of R_R. If centrifugal forces are neglected, the value for the y axis in Table 3 becomes

$$F_{TOTAL} = 108.33 \times 10^{-4} \text{ N} \quad .$$

These values represent the worst case from the standpoint of using the thrusters to their maximum value if centrifugal requirements are not considered. In the y axis, there are two thrusters with peak outputs of 65×10^{-4} N; therefore, the maximum y axis thrust is 130×10^{-4} N. The force available to compensate for the centrifugal forces is

$$F_{AV} = (130 - 108.33) \times 10^{-4} = 21.67 \times 10^{-4} \text{ N} \quad .$$

Thruster force required to counteract centrifugal forces is given by

$$F_c = M_v \omega_s^2 R_R \quad , \tag{22}$$

where M_v is the total mass of the vehicle. Varying the spin rate and radial offset, equation (22) has been plotted and is shown in Figure 12. Figure 13 is constructed by holding the spin rate constant at its nominal value (ω_s = 0.01047 rad/sec) and varying the radial offset. If the assumption is made that only one-half of the available force will be used for centrifugal purposes then

$$F_{AV} = \frac{21.67 \times 10^{-4}}{2} = 10.84 \times 10^{-4} \quad .$$

From Figure 13 the value of offset requiring this force is

$$R_R = 4.6 \text{ mm} \quad .$$

After choosing the conservative round off value the maximum radial offset has been set at 4 mm.

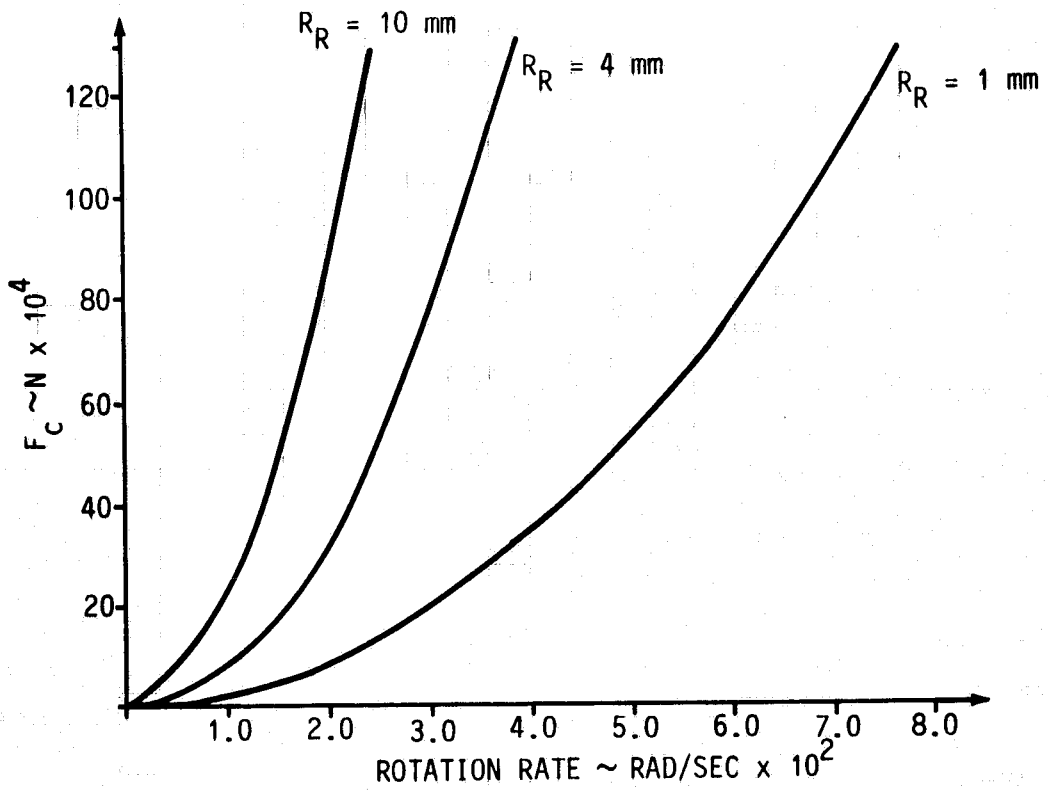

Figure 12. Centrifugal force requirement as a function of radial offset and rotation rate.

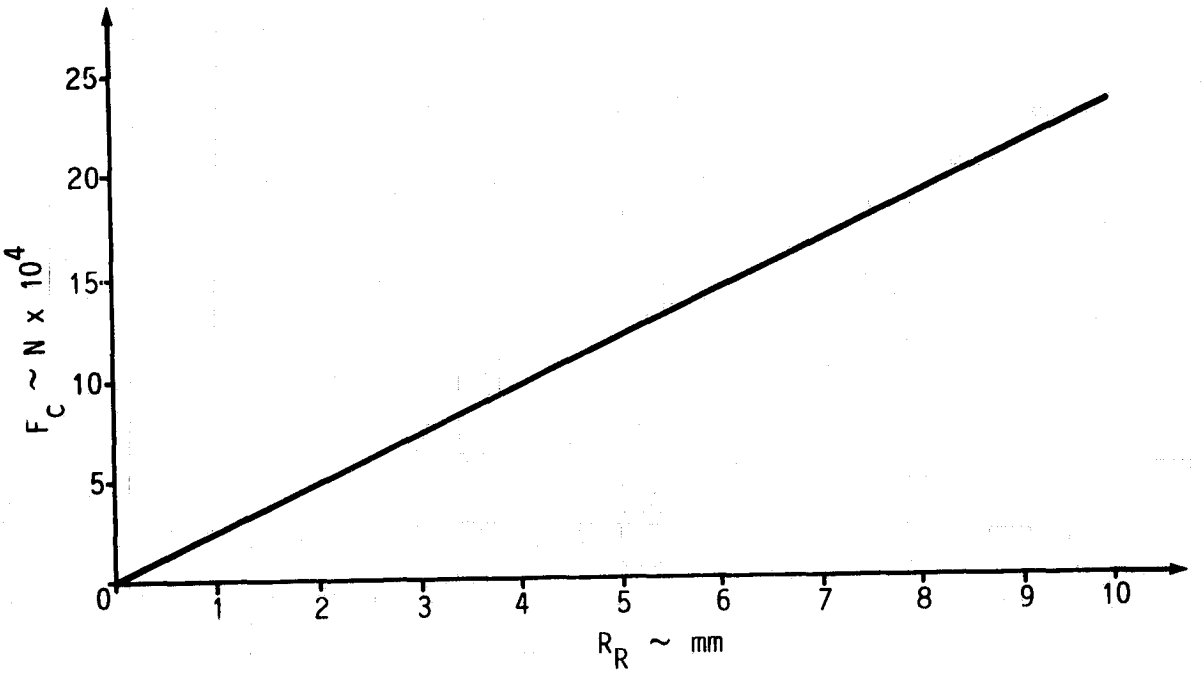

Figure 13. Centrifugal force requirement for nominal spin rate.

The direction of the offset becomes important when calculating the total amount of force necessary to meet the requirement. Figure 14 shows the offset at 45 deg to the pitch and yaw vehicle axes. This configuration represents the worst case and requires the vehicle to expend 15.34 x 10^{-4} N in order to meet the 10.84 x 10^{-4} N centrifugal requirement. For this reason the offset was chosen at 45 deg for the thruster sizing and total thrust requirement studies.

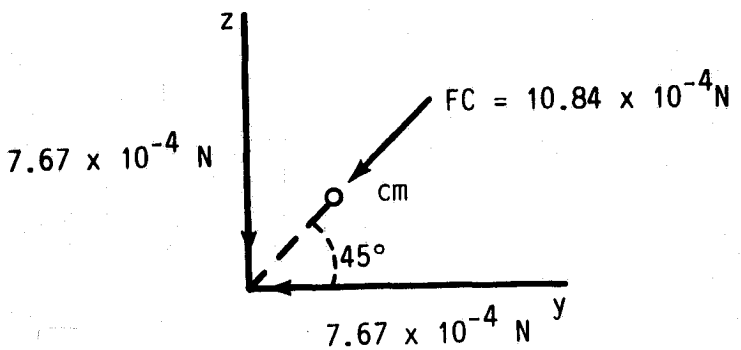

Figure 14. Center of mass offset in pitch and yaw axes.

Mass Balance

Fabricating the spacecraft with the precision to insure that the center of mass is within 4 mm of the proof mass may be a very difficult task. For this reason, a proposal has been made to incorporate a mass balance system in the vehicle design. Although several designs have been examined, no particular design has been chosen for GP-B at this time. For the purpose of discussion, in this report it will be assumed that masses can be moved onboard the vehicle to move the center of mass location in a radial direction only.

In order to correct the CM location a method must first be found to measure its present location. After the initial adjustment it is expected that the CM location will vary little and very slowly. For this reason, the control system will be operated in an open loop fashion. Appropriate data will be telemetered and the decision will be made by ground crews to command a CM adjustment. After the initial adjustment, only the use of propellants (liquid helium) and, to a lesser extent, solar array articulation can cause a CM movement.

From equation (22) the radial CM offset is given by

$$R_R = \frac{F_c}{M_v \omega_s^2} \quad . \tag{23}$$

If it is assumed that F_c is known to ±10 percent, M_v is known to ±5 percent, and ω_s is known to ±1 percent, then the upper bound on R_R is given by

$$R_u = \frac{1.1\ F_c}{(0.95\ M_v)(0.99\ \omega_s)^2} = 1.18\ R_R \text{ or } +18 \text{ percent} \quad .$$

The lower bound is then

$$R_L = \frac{0.9\ F_c}{(1.05\ M_v)(1.01\ \omega_s)^2} = 0.84\ R_R \text{ or } -16 \text{ percent} \quad .$$

A center of mass correction would then be made when the telemetered data indicated that the offset magnitude had reached a value of

$$R_R = \frac{4 \text{ mm}}{1.18} = 3.39 \text{ mm}$$

and adjusted to a value as close as possible to zero.

The assumed accuracies on M_v and ω_s are chosen purposefully to be conservative because it is not known just how accurately F_c can be determined. The difficulty arises from the fact that centrifugal forces must be separated from the forces caused by other disturbances.

At two points during each orbit the atmospheric drag forces are directed along the pointing axis of the vehicle. Centrifugal forces are perpendicular to this axis and remain body fixed as the spacecraft rotates. The force commands from the drag-free controller in the pitch and yaw axes approximate the

centrifugal forces during these periods and can be used to calculate F_c by equation (22). The values of the pitch and yaw components can be used to calculate the angular position of the CM. Appropriate commands can now be generated to shift the onboard masses and bring the center of mass within the 4 mm limit.

This is a very simple method for determining the CM location. Work in this area will continue to determine if more sophisticated methods exist to produce more exact results.

Nominal or Pointing Mode

After the fast spin mode has been attained and held for the length of time necessary to seat the helium, the vehicle's spin rate can be reduced to its nominal value of 0.0105 rad/sec. Vehicle pointing has already occurred and the drag-free control system can now be activated. The spin vector now shifts to the proof mass and any measurements necessary for center of mass determination can be taken. After center of mass corrections have been made, the dither signal can be introduced. The exact method of attaining the dither signal is still a subject of trade studies. Two possibilities will be briefly discussed here.

1. Inner Gimbal Control System – If this system is used, the canister containing the instrument will be gimbaled at the aft end of the dewar. Control is accomplished by means of piezoelectric actuators which gimbal the unit relative to the spacecraft and only in the pitch and yaw vehicle axes. In each axis the maximum angle of rotation will be on the order of 1 arc sec. The primary purpose of this system is to achieve the required 0.03 arc sec circular dither of the telescope pointing axis about the line-of-sight. There are several advantages to be gained if future studies indicate that this system can be eliminated:

a) The ACS control logic will be considerably simplified.

b) Spin-up gases from the experiment gyroscopes must cross the interface of the inner dewar and spacecraft to reach the nonpropulsive vents. If gimbaling occurs, bellows must be placed in each of these exhaust lines to compensate for the relative movement.

c) Motion of the instrument displaces the proof mass cavity and introduces coupling between the inner gimbal and the drag-free control system. This could prove to be a disadvantage when measuring the centrifugal forces since they each contribute to thruster commands perpendicular to the long vehicle axis.

d) The spacecraft would obviously be cheaper and easier to fabricate without this system.

2. Spacecraft Dither – The ACS would be used to dither the entire spacecraft normal to the line-of-sight. The dither signal is obtained by imposing the sinusoidal signals shown in Figure 15(a) on the vehicle pitch and yaw axes. Figure 15(b) shows the response of the vehicle in each axis and Figure 16 presents the net result to the pointing axis. The pointing axis can be made to rotate in either direction about the line-of-sight simply by reversing the signals applied to the y and z axes. This method of dither requires that the spacecraft structure between the thruster force application point and the rotation of the pointing axis be linear. It also requires that the thruster quantization and noise levels, as well as the vehicle dynamic characteristics, meet strict requirements. These will be discussed later.

Another requirement that must be met by the ACS in all modes of operation is the nonpropulsive venting of gaseous helium not used for control. This gas is boiled away from the dewar and is

completely separated from the spin-up gas supply. Past experience indicates that this function can best be accomplished by utilizing the thrusters used for control. The control thrusters are configured in opposing fashion (Fig. 1) and will eliminate the need for additional nonpropulsive vents.

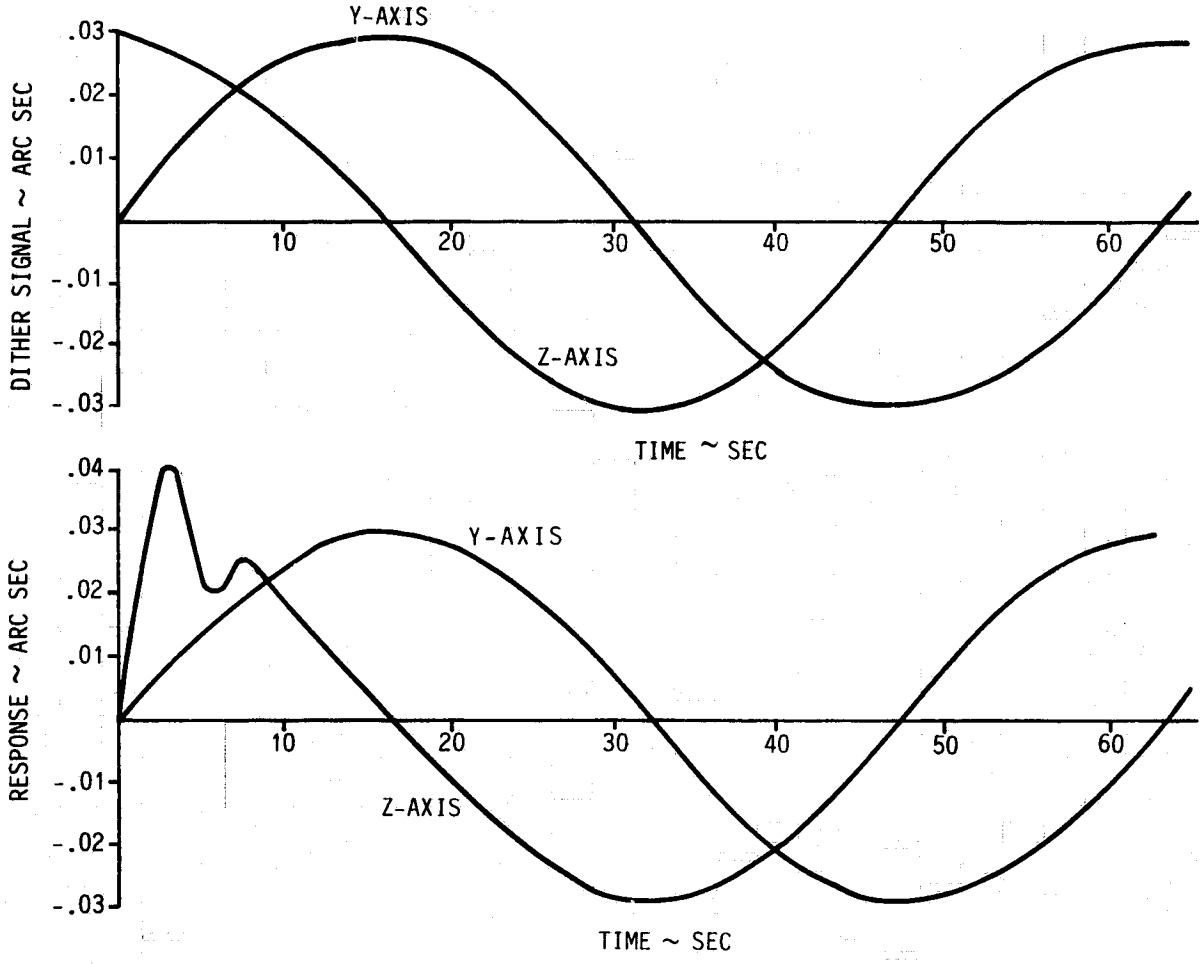

Figure 15. Pitch and yaw dither signals and vehicle computer model response.

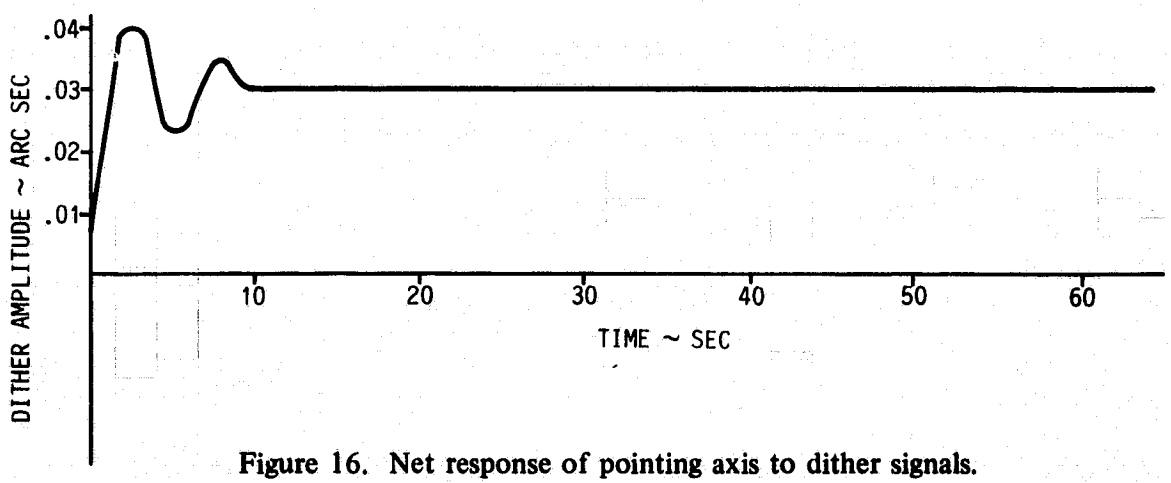

Figure 16. Net response of pointing axis to dither signals.

Reacquisition

In order to rotate the vehicle pointing axis through some large angle (out of the star tracker range) it is first necessary to determine the magnitude and direction of the desired maneuver.

The location of the guide star Rigel relative to the Earth fixed inertial frame is known throughout the entire mission lifetime. The Euler transformation matrix

$$[RE] = \begin{bmatrix} b_{11} & b_{12} & b_{13} \\ b_{21} & b_{22} & b_{23} \\ b_{31} & b_{32} & b_{33} \end{bmatrix} \tag{24}$$

can be determined at any time and used to relate inertial quantities to the guide star reference frame.

The orientation of the vehicle relative to the inertial frame is specified by the matrix

$$[VE] = \begin{bmatrix} a_{11} & a_{12} & a_{13} \\ a_{21} & a_{22} & a_{23} \\ a_{31} & a_{32} & a_{33} \end{bmatrix} \tag{25}$$

and must be determined by onboard optical sensors or by continuously updating the matrix by using the outputs from the body fixed rate gyroscopes.

The directional cosines of the X vehicle (pointing) axis relative to the inertial frame are specified by the first row of the [VE] matrix. Therefore the unit vector lying along the pointing axis is given by

$$a = a_{11}\, i + a_{12}\, j + a_{13}\, k \quad . \tag{26}$$

Likewise the unit vector pointing to the guide star is specified in the inertial frame by

$$b = b_{11}\, i + b_{12}\, j + b_{13}\, k \quad . \tag{27}$$

The vehicle control system must produce the torques necessary to rotate the vector a into the vector b. The problem in accomplishing this is mainly one of defining the commanded body rates (i.e., reference frame rates) in such a manner that the thrusters are not saturated.

The angular rotation and the inertial direction of the reference frame rates are defined by the vector cross product

$$a \times b = |a|\,|b| \sin\theta\, \bar{n} \quad , \tag{28}$$

where

θ = angle between a and b (radians)

$\bar{n}$ = unit vector in direction of a x b .

The angle θ is given by

$$\theta = \sin^{-1} |a \times b| \quad , \tag{29}$$

since $|a| = |b| = 1$.

The unit vector $\bar{n}$ is perpendicular to both a and b and is defined by

$$\bar{n} = \frac{a \times b}{|a \times b|} \quad . \tag{30}$$

The magnitude of the rotation (θ) and the direction of the reference frame rates ($\bar{n}$) are calculated only one time at the beginning of the rotation. Once the direction $\bar{n}$ has been calculated it remains inertially fixed throughout the rotation regardless of the intermediate positions of the spacecraft. Only the magnitude of the reference rates (ω_R in Fig. 17) will vary.

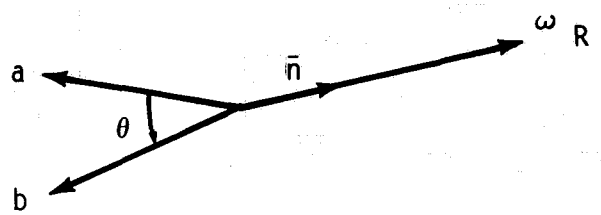

Figure 17. Vector relationship for pointing axis and guide star.

CASE I. In order to rotate through the angle θ in the smallest time, the general shape of ω_R is chosen to be as shown in Figure 18.

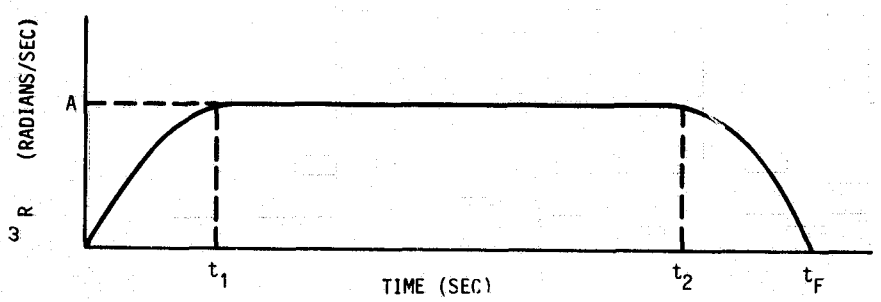

Figure 18. Reference frame rate for large angle maneuvers.

The curve in Figure 18 can be described by:

a) $0 \leqslant t \leqslant t_1$

$$\omega_R = A \sin \omega_N t$$

b) $t_1 < t < t_2$

$$\omega_R = A \qquad (31)$$

c) $t_2 \leqslant t \leqslant t_F$

$$\omega_R = A \sin [\pi/2 + \omega_N(t - t_2)]$$

d) $t > t_F$

$$\omega_R = 0 \quad .$$

The area under the curve is equal to the angle θ and is given by

$$\theta = 2 \int_0^{t_1} A \sin \omega_N t \, dt + A(t_2 - t_1) = A \left(\frac{2}{\omega_N} + t_2 - t_1 \right) \quad . \qquad (32)$$

From equation (31a) when $t = t_1$

$$\omega_R = A \quad .$$

Therefore $\omega_N t_1 = \pi/2$ and

$$\omega_N = \frac{\pi}{2 t_1} \quad . \qquad (33)$$

Substitution of equation (33) into equation (32) gives

$$\theta = A \left[\left(\frac{4}{\pi} - 1 \right) t_1 + t_2 \right] \quad . \qquad (34)$$

Differentiation of equation (31a) produces the angular acceleration

$$\dot{\omega}_R = A\ \omega_N \cos \omega_N t \quad . \tag{35}$$

The reference frame is accelerating only during zones (a) and (c) in Figure 18 giving an angular acceleration profile as shown in Figure 19.

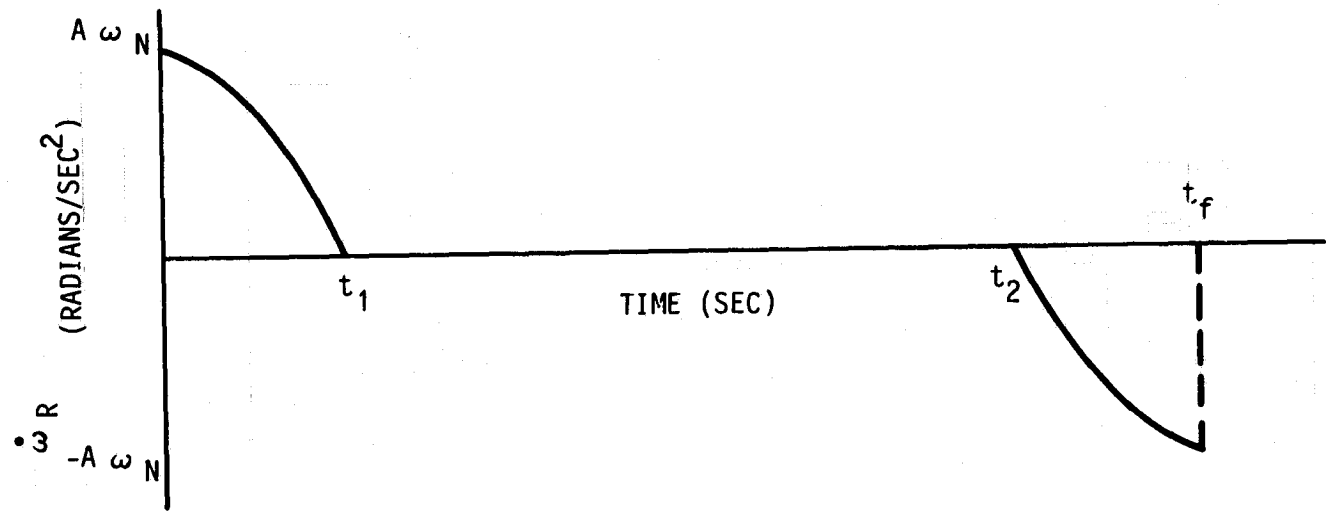

Figure 19. Reference frame acceleration for large angle maneuvers.

The Euler equation for angular rotation is

$$T = I\ \dot{\omega}_V + (\omega_V \times H) \quad , \tag{36}$$

where

I = moment of inertia about torque axis (kg-m^2)

T = resultant torque applied to the vehicle (N-m)

ω_V , $\dot{\omega}_V$ = vehicle angular rate and acceleration (rad/sec + rad/sec^2)

H = resultant momentum (kg-m^2/sec) .

If the assumption is made that the vehicle essentially follows the reference frame movement then equation (36) becomes

$$T = I\ \dot{\omega}_R + (\omega_R \times H) \quad . \tag{37}$$

If the spacecraft is in the nominal mode of operation the momentum vector lies along the X vehicle axis and

$$H = I_X \omega_X \quad . \tag{38}$$

Using equations (31a), (34), and (37) produces

$$T = A\, I\, \omega_N \cos \omega_N t + A\, I_X\, \omega_X \sin \omega_N t = T_1 + T_2 \quad . \tag{39}$$

The second term in equation (39) occurs 90 deg away from the first term (Fig. 20) and is initially non-existant.

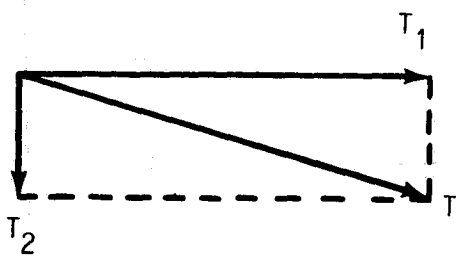

Figure 20. Euler torque components.

At time t = 0 all of the allotted torque can be directed into the angular acceleration of the vehicle and

$$T = T_1 = A\, I\, \omega_N \quad . \tag{40}$$

After the vehicle accelerates to its maximum angular velocity, the allotted torque is all directed into maintaining the rotation and

$$T = T_2 = A\, I_X\, \omega_X \quad . \tag{41}$$

Equation (40) and (41) gives

$$\omega_N = \frac{I_X\, \omega_X}{I} \quad . \tag{42}$$

Using equations (33) and (42) produces

$$t_1 = \frac{\pi I}{2 I_X \omega_X} \quad . \tag{43}$$

Now

$$t_2 = t_f - t_1 \quad , \tag{44}$$

and from equation (41)

$$A = \frac{T}{I_X \omega_X} \quad . \tag{45}$$

Substituting equations (43), (44), and (45) into equation (34) and solving for t_f yields

$$t_f = (\pi - 2) \frac{I}{I_X \omega_X} + \frac{\theta}{T} I_X \omega_X \quad , \tag{46}$$

and from (43), (44), and (46)

$$t_2 = \theta \frac{I_X \omega_X}{T} - \left(\frac{4 - \pi}{2}\right) \frac{I}{I_X \omega_X} \tag{47}$$

Using equation (4) to compute the inertial torque requirement, all parameters for maneuvering the vehicle can now be calculated with the guarantee that the total thruster output used in rotating the vehicle will not exceed

$$F_{TOTAL} = F_{MAX} P_C \quad . \tag{48}$$

The inertial torque (T) in Case I has a constant magnitude (after the initial transients have died out) and rotates in inertial space from its initial position to 90 deg in zone (a) of Figure 18, maintains its position at 90 deg through zone (b), and continues its rotation to 180 deg in zone (c).

CASE II. A degeneration of Case I occurs when $t_1 = t_2$ and therefore $t_f = 2t_1$. The profile in Figure 18 reduces to a pure sine wave described by equation (8a). Setting equation (43) equal to equation (47) and solving for T gives

$$T = \frac{(I_X \omega_X)^2}{2 I} \theta \quad . \tag{49}$$

Equation (32) reduces to

$$\theta = \frac{2A}{\omega_N} \quad . \tag{50}$$

Substituting equation (42) into equation (50) and solving for A gives

$$A = \frac{I_X \omega_X}{2I} \theta \quad . \tag{51}$$

Equation (43) gives the value for t_1 and

$$t_f = 2t_1 = \frac{\pi I}{I_X \omega_X} \quad . \tag{52}$$

A further generalization can be made when the left side of equation (49) [as calculated from equation (4)] is greater than the right side, i.e.,

$$T = \frac{F_{MAX} L P_C}{1.414} > \frac{(I_X \omega_X)^2}{2I} \theta \quad . \tag{53}$$

For this case the addition of a constant multiplier K will complete the equality and

$$T = \frac{(I_X \omega_X)^2}{2I} K \theta \quad . \tag{54}$$

Solving for Kproduces

$$K = \frac{2 I T}{(I_X \omega_X)^2 \theta} \quad . \tag{55}$$

Equation (39) now becomes

$$T = K\,A\,I\,\omega_N \cos \omega_N t + K\,A\,I_X\,\omega_X \sin \omega_N t \quad . \tag{56}$$

When $t = 0$

$$T = K\,A\,I\,\omega_N = I\,(\sqrt{K}\,A)\,(\sqrt{K}\,\omega_N) \quad . \tag{57}$$

where $\sqrt{K}\,A$ and $\sqrt{K}\,\omega_N$ are the new values of A and ω_N respectively. Separating K into its root values as in equation (57) preserves the value of θ since

$$\theta = \frac{2\sqrt{K}\,A}{\sqrt{K}\,\omega_N} = \frac{2A}{\omega_N} \tag{58}$$

Now from equation (33)

$$\sqrt{K}\,\omega_N = \frac{\pi}{2t_1} \quad , \tag{59}$$

and

$$t_1 = \frac{\pi}{2\sqrt{K}\,\omega_N} \quad . \tag{60}$$

Therefore

$$t_f = 2t_1 = \frac{\pi}{\sqrt{K}\,\omega_N} = \frac{\pi\,I}{\sqrt{K}\,I_X\,\omega_X} \quad . \tag{61}$$

The values of ω_N and A now become

$$\omega_N = \frac{\sqrt{K}\,I_X\,\omega_X}{I} \quad ; \quad A = \frac{\sqrt{K}\,I_X\,\omega_X}{2I}\,\theta \quad , \tag{62}$$

giving

$$\omega_R = \frac{\sqrt{K}\, I_X\, \omega_X}{2I}\, \theta \sin \frac{\sqrt{K}\, I_X\, \omega_X}{I}\, t \quad , \tag{63}$$

for

$$0 \leqslant t \leqslant \frac{\pi\, I}{\sqrt{K}\, I_X\, \omega_X} \quad .$$

Case II will apply when the guide star is within the field of view of the star tracker. The initial value of θ will be determined from the star tracker output and the vehicle will follow the reference frame rotation given by equation (63). When the rotation is complete another value of θ will be determined from the star tracker and, if needed, the process will be repeated.

In general if $K < 1$ Case I will apply and the reference frame rate will be as shown in Figure 18. If $K \geqslant 1$ then Case II will apply with a reference frame rate as described in equation (63).

Figure 21 shows the time required to rotate the vehicle through various large angles assuming 50 percent of the maximum ($P_C = 0.5$) thrust is available for maneuvering. Equation (46) applies when $K < 1$ and equation (61) is used when the guide star is within the star tracker field of view and $\theta \leqslant$ 0.0736 rad ($K \geqslant 1$).

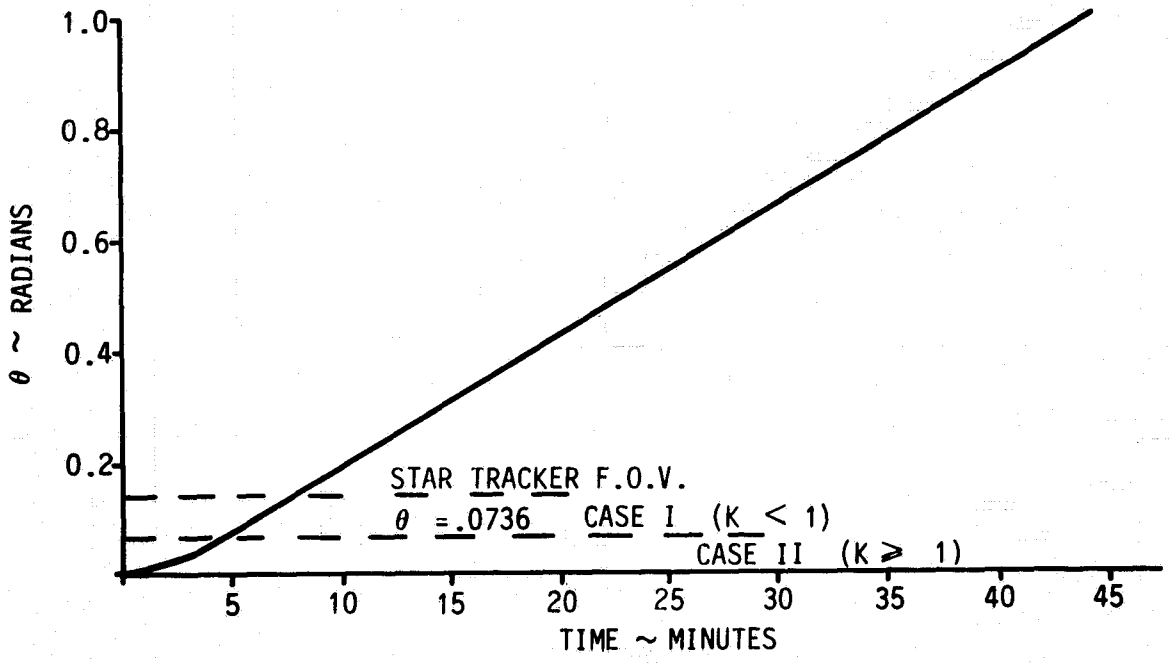

Figure 21. Time requirement for large angle maneuvers.

CONTROL SYSTEMS BLOCK DIAGRAM AND FUNCTIONS

Figure 22 presents a simplified block diagram of the various control systems onboard the Gravity Probe-B spacecraft. Each sensor, actuator, and computer function will be discussed briefly.

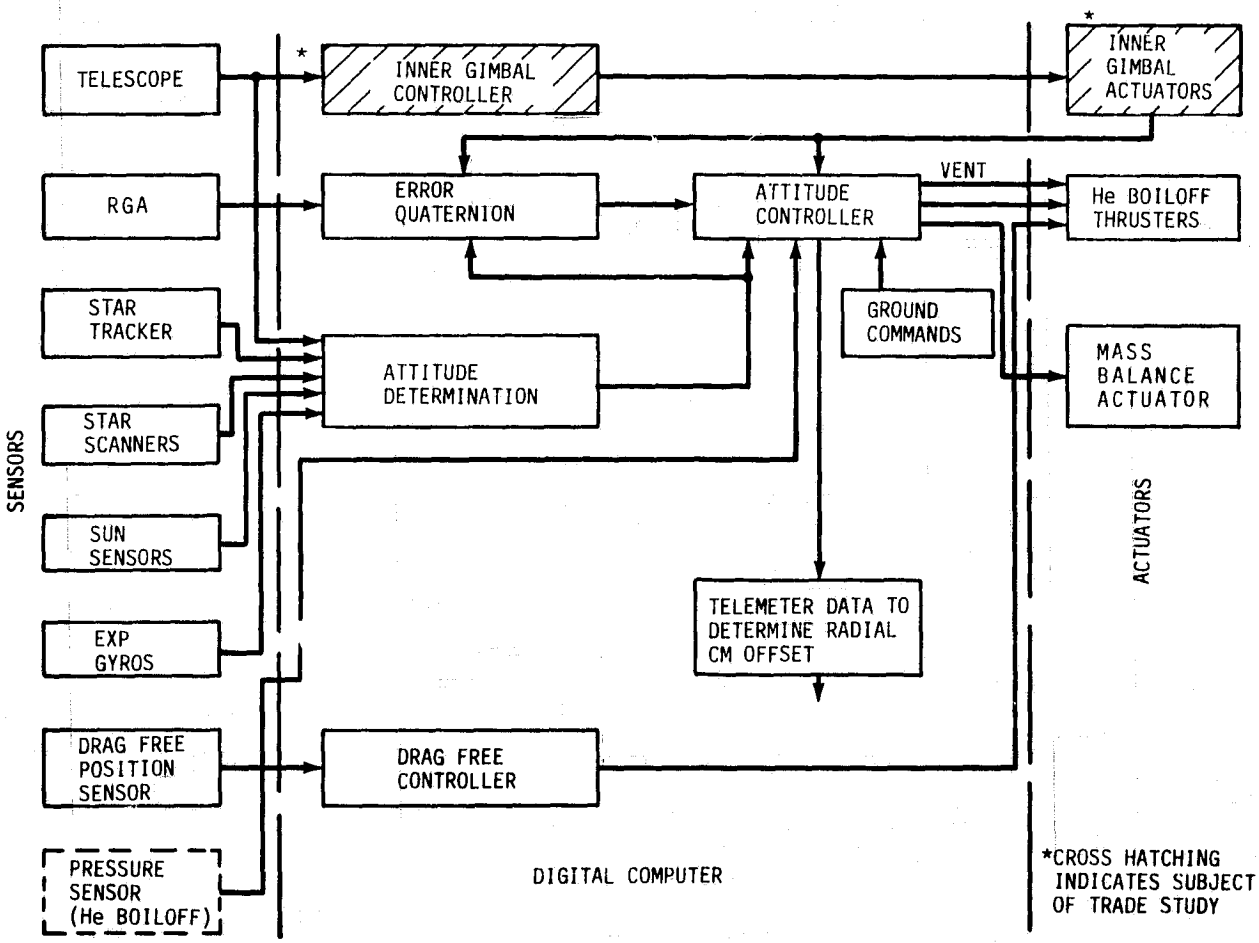

Figure 22. Control systems – simplified block diagram.

SENSORS

Telescope

The telescope is an integral part of the instrument unit, and its line-of-sight is aligned as closely as possible with the experiment gyros and the center of the proof mass cavity. For the present control studies it was assumed that the telescope output axes were exactly aligned with the vehicle pitch and yaw axes. The telescope produces four signals which represent the intensity of the guide star image along the ±y and ±z spacecraft axes. The characteristics of the telescope for one of these signals is shown in Figure 23. Up to 0.05 arc sec the signal produced is exactly proportional to the angle of deviation from the

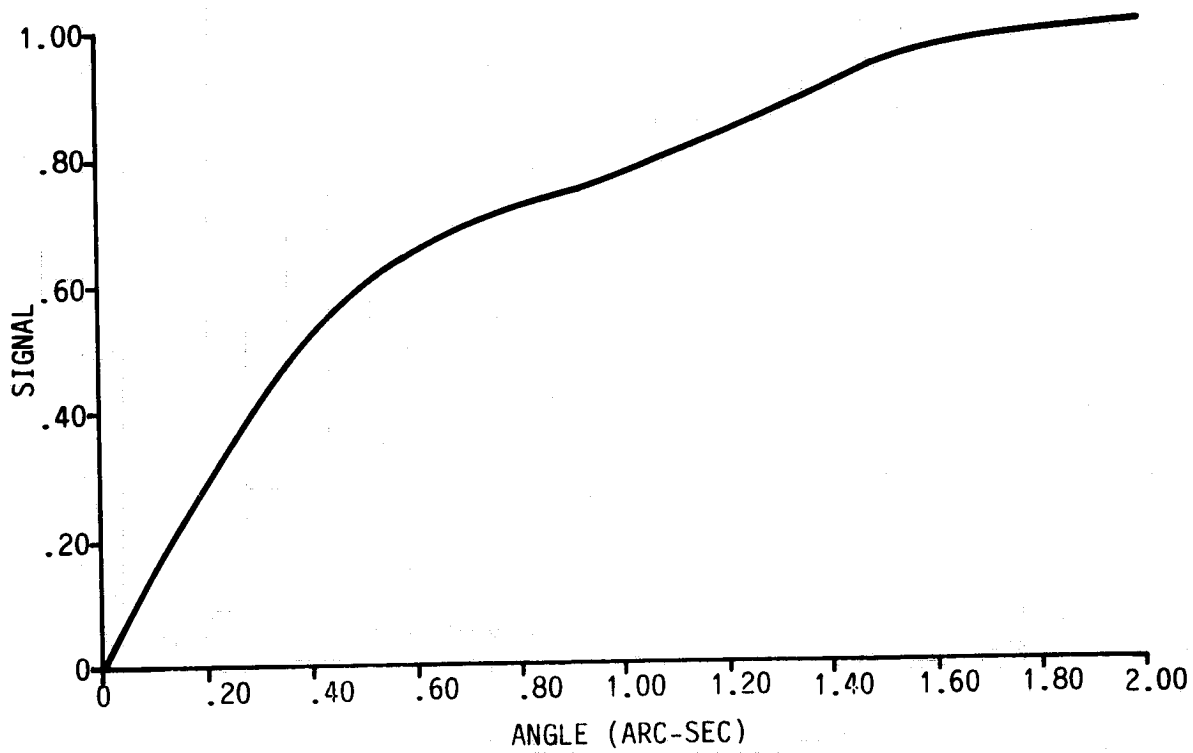

Figure 23. Intensity of telescope signal as a function of pointing error.

star image. The intensity reaches its maximum at 2 arc sec and remains constant until the signal drops out at approximately 2 arc min. The telescope outputs and the rate of change of the outputs are used to generate the rate and error signals for input to the control algorithm. No roll axis information is derived from the telescope. The pitch and yaw signals are used to drive the star image to a point where the intensities are equal for all outputs.

Star Trackers

Redundant star trackers will be used. Each sensor has an 8 by 8 deg field-of-view and will be used for control purposes in the same manner as the telescope. While the telescope acquires the guide star the primary purpose of the star tracker is to provide the signals to rotate the vehicle to a pointing accuracy within the telescope field-of-view. Once this has been accomplished the star trackers will be used only as necessary for reacquisition or possibly in a search mode if for some reason the vehicle becomes lost.

Rate Gyroscope Assembly (RGA)

Redundant rate gyros will be utilized in all three vehicle axes. The RGA signals will be used for vehicle control in the roll axis throughout the entire mission. Pitch and yaw information from the RGA's will be used to rotate the guide star into the star tracker field-of-view during initial acquisition if necessary and for any large angle maneuver when the guide star is not present. All RGA's must remain active until the experiment gyroscopes have reached their final spin speed.

Experiment Gyros

The guide star is occluded by the Earth once each orbit. As an energy saving measure the present mission plan calls for operating the pitch and yaw rate gyros in a reduced power state only after the relativity gyros have reached spin speed. During guide star occlusion the experiment gyro outputs will be used to obtain the rate signals necessary for control.

Sun Sensors

Sun sensors to provide a 4π steradian field-of-view will be located at various places around the spacecraft. These sensors will provide a course attitude determination for acquisition and reacquisition when the guide star is not within the star tracker field-of-view.

Star Scanners

The roll position of the instrument unit must be known to an accuracy of ±20 arc sec at all times when scientific data is being taken. Star scanners mounted such that their field-of-view is perpendicular to the telescope line-of-sight can be used to determine the spacecraft roll angle to the desired accuracy. For this reason provisions will be made to initially align the scanners with the instrument by optical methods. The star scanners will serve the dual purpose of providing an update or calibration for the roll axis rate gyroscopes and providing the beginning signal from which the roll angle will be measured, i.e., the roll angle is determined by

$$\theta = \omega_S \, \Delta\tau$$

where $\Delta\tau$ and, therefore, θ are measured from the scanner output signal.

Drag-Free Position Sensor

This sensor is capable of determining the three-dimensional offset of the proof mass to an accuracy of one microinch. The position and derived velocity of the proof mass are used in a control algorithm to attain the required average orbital acceleration.

Pressure Sensor (He Boil-Off)

This sensor is actually a part of the boil-off control system. It is used in the ACS to determine when excess helium should be vented nonpropulsively through the control thrusters. Venting will continue through selected thrusters until the gaseous helium pressure returns to predetermined limits.

ACTUATORS

Helium Boil-Off Thrusters

These actuators are used for attitude, drag-free, and nonpropulsive venting control. The original design of the spacecraft utilized thrusters which continuously vented through opposing nozzles. The required one year lifetime of the GP-B and the discovery that aerodynamic forces were considerably greater than originally thought necessitates the development of thrusters whose control gas output can be stopped when not in use.

The following is a list of thruster requirements:

1) Force output variable over the range of 0 to 65 x 10^{-4} N maximum.

2) The force generated by each thruster shall be the commanded value ±2 percent (steady state error).

3) The power spectral density of the force noise in the frequency range from 0 to 10 Hz shall be less than 10^{-12} N^2/Hz.

4) The thruster shall respond to commands of thrust changes of 10^{-6} N. This defines the thruster quantization and hysteresis.

5) The force (F) developed by each thruster will respond to the command (F_c) according to the dynamic transfer function

$$\frac{F}{F_c} = \frac{\omega^2}{s^2 + 2\zeta\omega S + \omega^2}$$

where $\omega = 2\pi f$ ($f \geqslant 10$ Hz) and $\zeta = 0.707$.

MASS BALANCE ACTUATORS

A system for mass balance control has not yet been selected. Several alternatives exist involving fluid transfer, tape spooling, and solid mass movement. This study will be carried forward into phase C-D where the optimum design will be selected and analyzed.

INNER GIMBAL ACTUATORS

The characteristics of these actuators have not yet been determined. The maximum extension will produce at least the dither requirement (0.03 arc sec) and respond to the dither frequency of 0.1 rad/sec. This also will be a trade item carried into phase C-D.

DIGITAL COMPUTER

The digital computer receives and processes the signals from the various sensors to achieve the desired vehicle control. Functions to be performed by the digital computer include:

1) Receive and execute ground commands.

2) Generate the torque and translation commands needed for attitude and drag-free control.

3) Perform signal filtering to insure adequate stability margins.

4) Insure nonpropulsive venting.

5) Quaternion integration for attitude control.

6) Issue the telescope dither commands.

7) Select the thrusters to be fired in response to control algorithm commands.

CONTROL PHILOSOPHY AND GAIN CALCULATIONS

A proportional, integral, and differential gain (PID) type control method was chosen for both the Attitude Control System (ACS) and the Drag-Free Control System (DFCS). This method of control is well within the state of the art and lends itself well to GP-B applications. The integral gain is especially useful in nulling very small telescope pointing errors and in keeping the proof mass centered in its cavity.

There are several methods for calculating the PID gains. Only one will be discussed here, but the best set of gains (regardless of method) will be selected in Phase C-D. Only the ACS will be shown here. The block diagram for the DFCS will be identical except for replacing inertia terms with vehicle mass.

Figure 24 represents the ACS rigid body for a single axis. The following definitions apply:

T_D = disturbance torque (N·m)

T_{con} = torque applied by control thrusters (N·m)

T_R = resultant torque as seen by the vehicle (N·m)

I = vehicle inertia about a single axis (kg-m^2)

G_P = proportional control gain (N·m)

G_I = integral control gain (N·m/s)

G_D = differential control gain (N·m·s)

S = LaPlace operator (1/s)

T_c = commanded torque (N·m) .

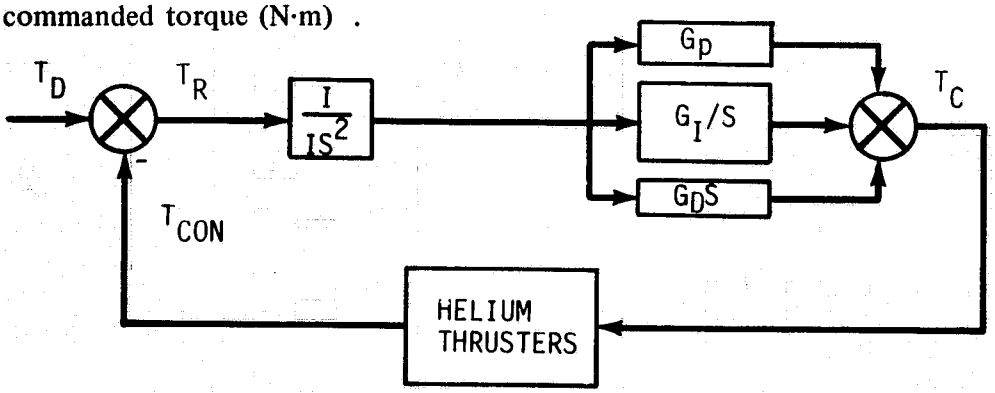

Figure 24. ACS rigid body block diagram.

Writing the transfer function from disturbance to command and simplifying gives

$$\frac{T_c}{T_D} = \frac{G_D S^2 + G_P S + G_I}{I S^3 + G_D S^2 + G_P S + G_I} \quad .$$

Setting the characteristic equation to zero and dividing by the vehicle inertia gives

$$S^3 + \frac{G_D S^2}{I} + \frac{G_P S}{I} + \frac{G_I}{I} = 0 \quad .$$

Gain calculations are made by setting the above equation equal to the product of a second order equation dependent only upon the control parameters and a first order equation determined by the integral gain. Thus

$$S^3 + \frac{G_D S^2}{I} + \frac{G_P S}{I} + \frac{G_I}{I} = (S^2 + 2\zeta_c \omega_c S + \omega_c{}^2)\,(S + \omega_I)$$

where

ω_c = control frequency (rad/sec)

ζ_c = damping ratio (unitless)

ω_I = integral loop frequency (rad/sec) .

After multiplying and equating coefficients of like powers, the following relationships can be derived:

$$G_D = I(\omega_I + 2\zeta_c \omega_c)$$

$$G_P = I(\omega_c{}^2 + 2\zeta_c \omega_c \omega_I)$$

$$G_I = I\,\omega_c{}^2 \omega_I$$

In practice, it is common to assume the control and integral frequencies to be related by (K is a constant)

$$\omega_I = K\omega_c$$

If this substitution is made, the gain equations are

$$G_D = I\omega_c(2\zeta_c + K)$$

$$G_P = I\omega_c^2(1 + 2K\zeta_c)$$

$$G_I = I\omega_c^3 K$$

for attitude control and

$$G_D = M_V\omega_c(2\zeta_c + K)$$

$$G_P = M_V\omega_c^2(1 + 2K\zeta_c)$$

$$G_I = M_V\omega_c^3 K$$

for drag-free control. Choosing

$$K = 0.1$$

$$\omega_c = 0.6283 \text{ rad/sec } (F_c = 0.1 \text{ Hz})$$

$$\zeta_c = 0.707$$

and the GP-B mass and inertia characteristics as specified in memo EL51(24-82) for symmetrical helium and solar arrays in the 90 deg position produces the following gains for attitude control:

$G_{Dx} = 5149.6$ N·m·s $\quad G_{Px} = 2439.3$ N·m $\quad G_{Ix} = 134.3$ N·m/s

$G_{Dy} = 5050.5$ N·m·s ; $G_{Py} = 2392.3$ N·m ; $G_{Iy} = 131.7$ N·m/s

$G_{Dz} = 5050.7$ N·m·s $\quad G_{Pz} = 2392.4$ N·m $\quad G_{Iz} = 131.7$ N·m/s

where the subscripts x, y, z indicate a particular vehicle axis.

The drag-free gains are

$G_D = 2045$ kg/s

$G_P = 968.7$ kg/s^2

$G_I = 53.2$ kg/s^3

for all vehicle axes.

The response of the attitude control system to a small angle error about the roll axis is shown in Figure 25. The inertia tensor has been diagonalized to prevent cross-coupling into the pitch and yaw vehicle axes.

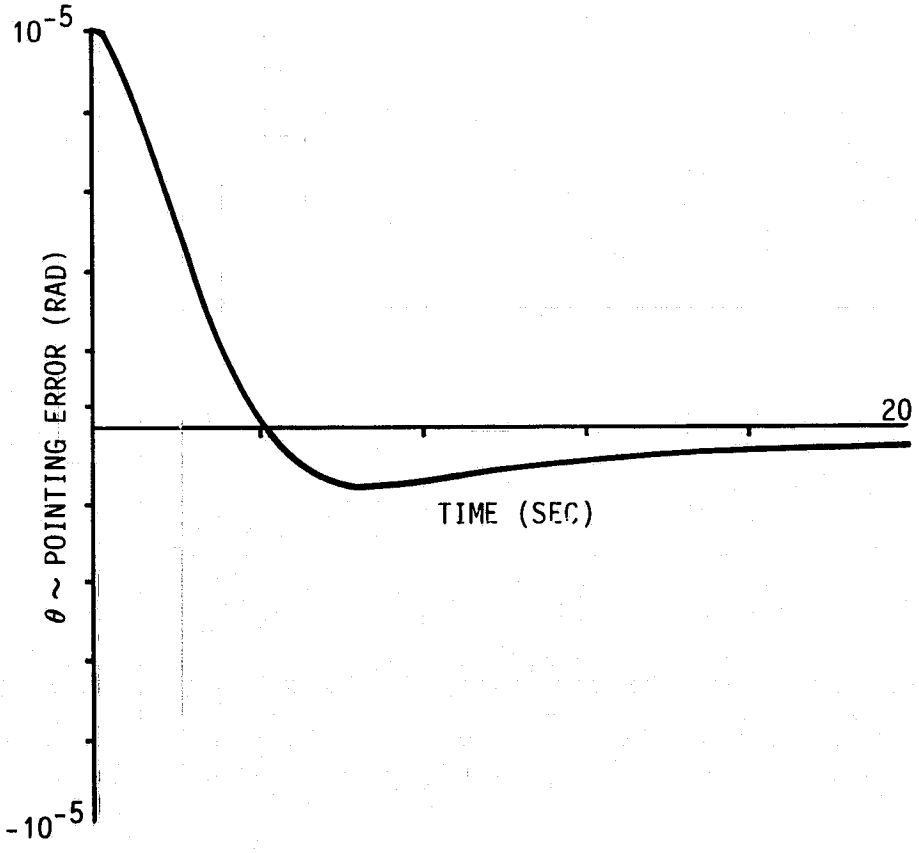

Figure 25. Attitude control system transient response.

Figure 26 shows a displacement of the proof mass (along the x axis) and the vehicle response to recenter the proof mass in its cavity. Again cross-coupling was prevented by making the center of mass coincident with the cavity center.

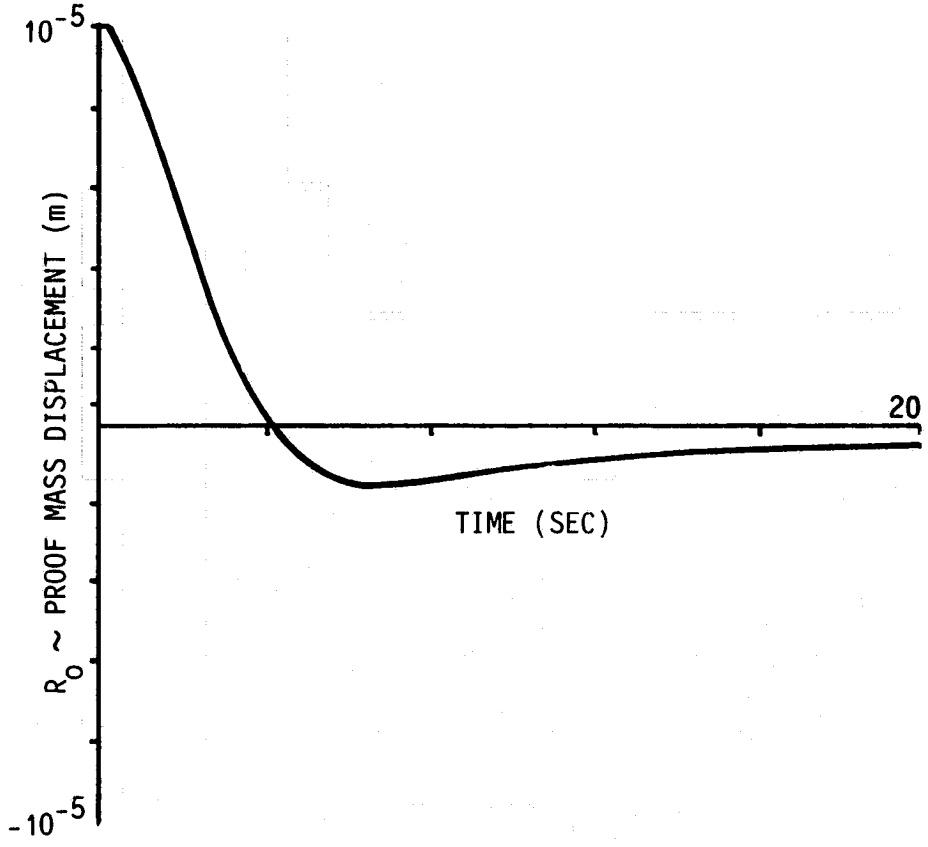

Figure 26. Drag-free control system transient response.

FUTURE STUDIES

a) Work will continue on the GP-B computer simulation. The time domain simulation will be expanded to include the flexible body characteristics of the four solar arrays and the suspension system of the cannister housing the instrument unit. Each component part of the control system (i.e., sensors, control algorithms, actuators, etc.) will be characterized and simulated. The computer program will then be used to:

1) Determine the vehicle response to various attitude and translational disturbance forces.

2) Adjust control gains and design filters to achieve the best stability margins and response times.

3) Perform error budget studies and failure mode analyses.

4) Aid in developing search mode techniques and methods of rotating the line-of-sight after the vehicle has reached spin speed.

Large angle commands to the vehicle pitch and yaw axes after spacecraft spin up presents special problems. The vehicle responds to attitude commands in the manner of a large gyroscope with its momentum vector parallel to the telescope line-of-sight. Equations to command the vehicle under these conditions have been developed, but have not yet been implemented.

b) Utilizing onboard sensors, methods should be developed to determine the spacecraft attitude if the vehicle becomes lost, i.e., the guide star is not within the star tracker field-of-view. The sun sensors provide one line of reference, but the best method of determining the orientation of the spacecraft about the sun line cannot be determined in an obvious manner.

c) The high degree of roll rate uniformity and the ±20 arc sec roll determination requirement may make it necessary to provide more than one signal from the star scanners during the course of one roll period. The roll determination is a requirement on the instrument unit and, therefore assumes that the initial alignment between the scanners and the instrument does not vary appreciably. Thermal deformations during the mission may make it practical to include an active determination of the scanner-instrument alignment.

d) If the inner gimbal control system is to be eliminated the mechanisms that transmit the thruster forces to the instrument unit must be linear. Included in this requirement are the solar array deployment and articulation devices and the suspension of the instrument cannister within the cryogenic dewar.

e) A detailed analysis of the interaction between the boil-off control system and the instantaneous thrust requirements of the attitude and drag-free control systems will be undertaken.

Each of the areas listed above will be the subject of future studies. The list is far from complete and will be extended and revised as the design matures.

APPROVAL

GRAVITY PROBE-B CONTROL SUBSYSTEM

By John Farmer

The information in this report has been reviewed for technical content. Review of any information concerning Department of Defense or nuclear energy activities or programs has been made by the MSFC Security Classification Officer. This report, in its entirety, has been determined to be unclassified.

GEORGE F. McDONOUGH
Director, Systems Dynamics Laboratory

☆ U.S. GOVERNMENT PRINTING OFFICE: 1983—646-058/168